Article

Cancer Cell

Glutathione and Thioredoxin Antioxidant Pathways Synergize to Drive Cancer Initiation and Progression

Graphical Abstract

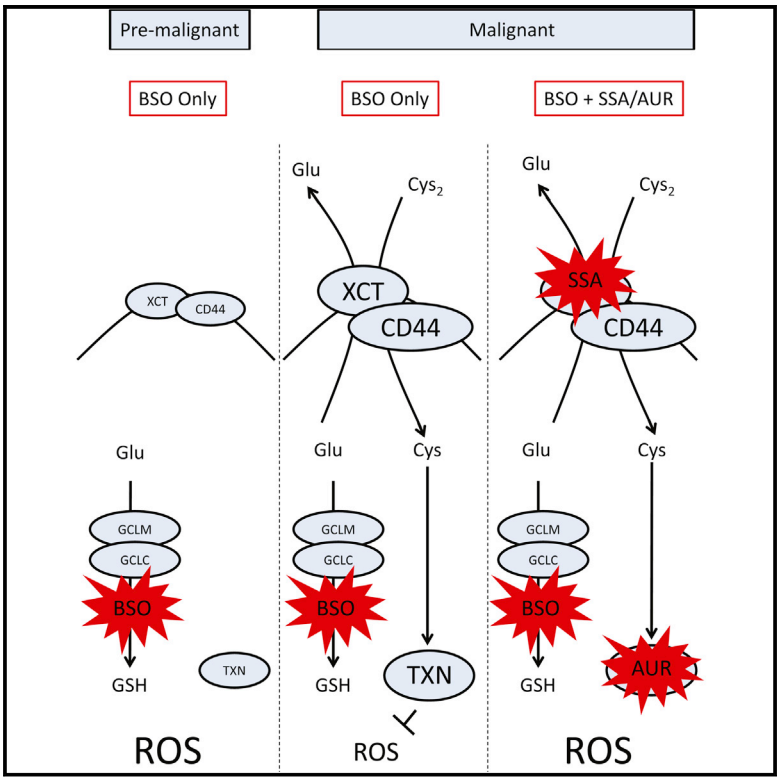

Highlights

- The GSH antioxidant pathway is required for cancer initiation
- After cancer initiation, GSH is dispensable due to alternative antioxidant pathways
- The TXN antioxidant pathway is upregulated in tumors
- Inhibition of both GSH and TXN pathways causes synergistic cancer cell death

Authors

Isaac S. Harris, Aislinn E. Treloar, ..., Ching-Wan Lam, Tak W. Mak

Correspondence

tmak@uhnres.utoronto.ca

In Brief

Harris et al. show that the antioxidant glutathione (GSH) is required for cancer initiation but not for established tumors partly due to upregulation of the thioredoxin (TXN) antioxidant pathway in the latter. Consequently, blocking both GSH and TXN pathways synergistically inhibits tumor growth.

Harris et al., 2015, Cancer Cell *27*, 211–222
February 9, 2015
http://dx.doi.org/10.1016/j.ccell.2014.11.019

CellPress

Cancer Cell
Article

Glutathione and Thioredoxin Antioxidant Pathways Synergize to Drive Cancer Initiation and Progression

Isaac S. Harris,[1,2,12] Aislinn E. Treloar,[1,2] Satoshi Inoue,[1] Masato Sasaki,[1,6] Chiara Gorrini,[1] Kim Chung Lee,[7] Ka Yi Yung,[7] Dirk Brenner,[1,8] Christiane B. Knobbe-Thomsen,[9] Maureen A. Cox,[1] Andrew Elia,[1] Thorsten Berger,[1] David W. Cescon,[1,2] Adewunmi Adeoye,[1,4,5] Anne Brüstle,[1] Sam D. Molyneux,[2,3] Jacqueline M. Mason,[1] Wanda Y. Li,[1] Kazuo Yamamoto,[10] Andrew Wakeham,[1] Hal K. Berman,[1,4,5] Rama Khokha,[2,3] Susan J. Done,[1,4,5] Terrance J. Kavanagh,[11] Ching-Wan Lam,[7] and Tak W. Mak[1,2,*]

[1]The Campbell Family Institute for Breast Cancer Research
[2]Department of Medical Biophysics
[3]Ontario Cancer Institute
[4]Laboratory Medicine Program
[5]Department of Laboratory Medicine and Pathobiology
University Health Network, 620 University Avenue, Toronto, ON M5G 2M9, Canada
[6]Department of Infection and Host Defense, Tohoku Pharmaceutical University, 4-4-1 Komatsushima, Aoba-ku, Sendai, Miyagi 981-8558, Japan
[7]Department of Pathology, The University of Hong Kong, Hong Kong, China
[8]Department of Infection and Immunity, Luxembourg Institute of Health, 84, Val Fleuri, 1526 Luxembourg, Luxembourg
[9]Department of Neuropathology, Heinrich Heine University, 40225 Düsseldorf, Germany
[10]Division of Cell Function Research Support, Biomedical Research Support Center, Nagasaki University School of Medical Sciences, 1-12-4 Sakamoto, Nagasaki 852-8523, Japan
[11]Department of Environmental and Occupational Health Sciences, University of Washington, Seattle, WA 98195, USA
[12]Present address: Department of Cell Biology, Harvard Medical School, 240 Longwood Avenue, Boston, MA 02115 USA
*Correspondence: tmak@uhnres.utoronto.ca
http://dx.doi.org/10.1016/j.ccell.2014.11.019

SUMMARY

Controversy over the role of antioxidants in cancer has persisted for decades. Here, we demonstrate that synthesis of the antioxidant glutathione (GSH), driven by GCLM, is required for cancer initiation. Genetic loss of *Gclm* prevents a tumor's ability to drive malignant transformation. Intriguingly, these findings can be replicated using an inhibitor of GSH synthesis, but only if delivered prior to cancer onset, suggesting that at later stages of tumor progression GSH becomes dispensable potentially due to compensation from alternative antioxidant pathways. Remarkably, combined inhibition of GSH and thioredoxin antioxidant pathways leads to a synergistic cancer cell death in vitro and in vivo, demonstrating the importance of these two antioxidants to tumor progression and as potential targets for therapeutic intervention.

INTRODUCTION

Reactive oxygen species (ROS) are normal byproducts of numerous cellular processes, such as mitochondrial metabolism and protein folding (Cairns et al., 2011). At low levels, ROS act as signaling molecules to activate proliferation and survival pathways (Sena and Chandel, 2012). At moderately increased levels, ROS damage DNA and promote mutagenesis in cells (Wiseman

Significance

Although supplementation with antioxidants has been suggested to prevent cancer, we show that inhibition of antioxidant synthesis can, in fact, be chemopreventive. Clinical trials using buthionine sulfoximine (BSO), which inhibits GSH synthesis, to treat malignancies have failed though, possibly due to the response from alterative antioxidant pathways such as the TXN pathway. We demonstrate that sulfasalazine (SSA) and auranofin (AUR), inhibitors of the TXN pathway currently used in clinics to treat inflammatory diseases, can be combined with BSO to reduce tumorigenesis. Combined inhibition of GSH and TXN pathways may be a valuable therapeutic strategy to treat cancer patients and one that can be readily implemented.

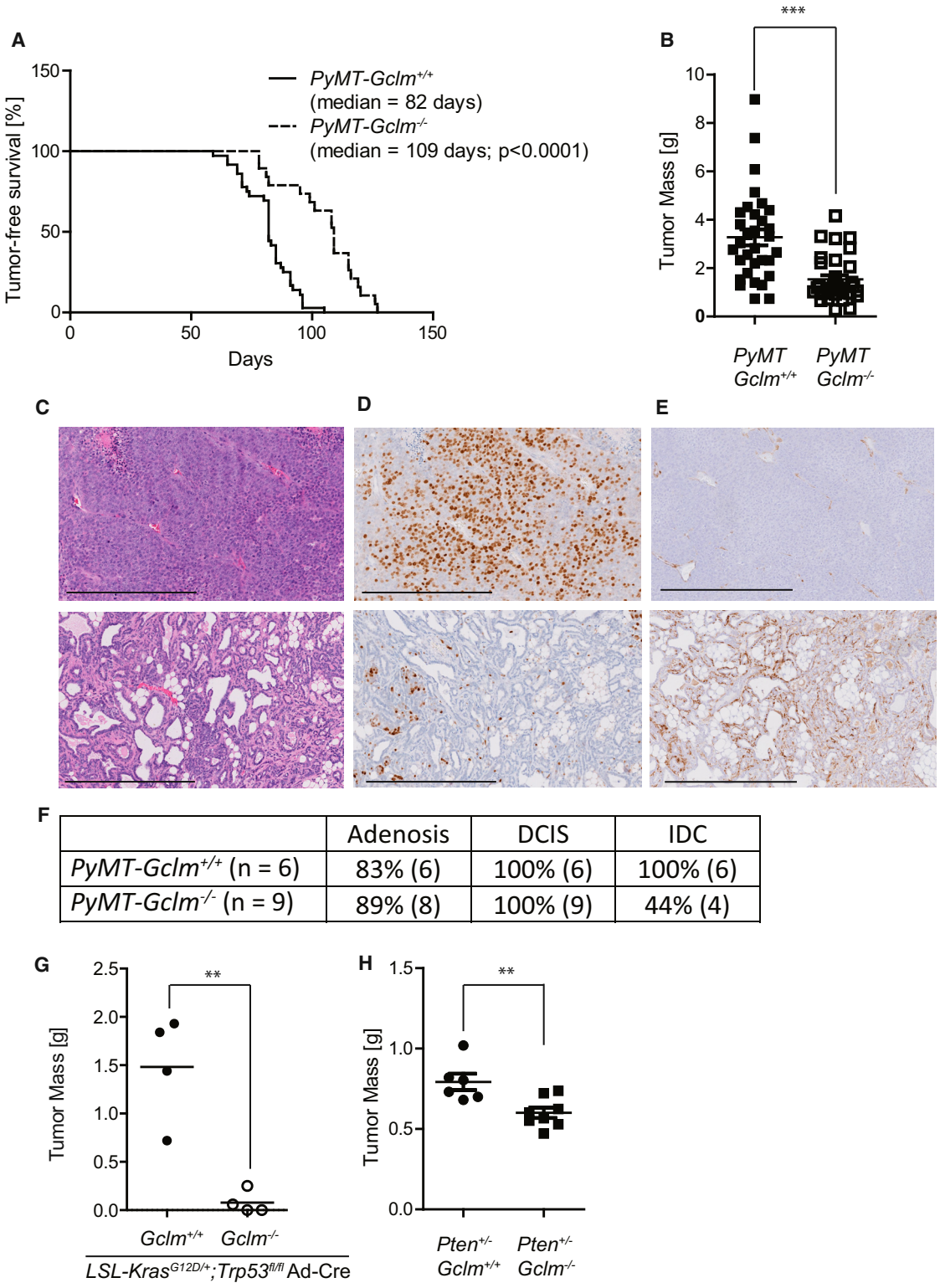

	Adenosis	DCIS	IDC
PyMT-Gclm$^{+/+}$ (n = 6)	83% (6)	100% (6)	100% (6)
PyMT-Gclm$^{-/-}$ (n = 9)	89% (8)	100% (9)	44% (4)

Figure 1. *Gclm* Is Required for Tumor Initiation

(A) Tumor-free survival of *PyMT-Gclm*$^{+/+}$ (n = 36) and *PyMT-Gclm*$^{-/-}$ (n = 19) mice.

(B) At the endpoint (day 160), all tumors from *PyMT-Gclm*$^{+/+}$ (n = 32) and *PyMT-Gclm*$^{-/-}$ (n = 32) mice were resected and weighed. Each data point represents the combined weight of tumors from a single mouse.

(C–E) Representative images of tumor sections from *PyMT-Gclm*$^{+/+}$ (top) and *PyMT-Gclm*$^{-/-}$ (bottom) mice stained for H&E (C), Ki67 (D), and smooth muscle actin (SMA) (E). Scale bars represent 400 μm.

(legend continued on next page)

and Halliwell, 1996). High ROS levels, however, exert an oxidative stress on the cell that can ultimately cause cell senescence or death (Trachootham et al., 2009). To control oxidative stress, cells generate molecules termed antioxidants that convert ROS into benign molecules.

The most abundant antioxidant within all cells is glutathione (GSH) (Meister, 1983). GSH is synthesized in a two-step process; the rate limiting step is carried out by glutamate cysteine ligase (GCL), a heterodimer of catalytic (GCLC) and modifier (GCLM) subunits. Gene-targeted GCLC-deficient (*Gclc*$^{-/-}$) mice lack all GSH synthesis and die during embryogenesis (Dalton et al., 2000). In contrast, *Gclm*$^{-/-}$ mice have only 10%–25% of the GSH levels of wild-type mice, but are completely viable (McConnachie et al., 2007). Although *Gclm*$^{-/-}$ mice have greatly reduced GSH synthesis, no overt phenotypes in relation to cancer have been observed.

Cancer cells arise from activation of oncogenes and/or inactivation of tumor suppressors. A key hallmark of cancer cells is unrestrained growth (Hanahan and Weinberg, 2000). Because generation of ROS is a byproduct of cell growth, cancer cells sustain a much higher level of ROS production compared to normal cells (Trachootham et al., 2006). Therefore, to avoid the detrimental effects of oxidative stress, it is believed that cancer cells must actively upregulate multiple antioxidant systems. By buffering ROS levels, cancer cells are able to restrict ROS within a range that is beneficial to promote tumor progression. Recent reports have proposed this hypothesis (DeNicola et al., 2011; Diehn et al., 2009; Schafer et al., 2009), yet the importance of antioxidants during tumor initiation and progression still remains to be tested. Here, we examine the impact of inhibiting the GSH antioxidant pathway on tumorigenesis.

RESULTS

The Role of GCLM in Tumorigenesis

In order to investigate the impact of GCLM on cancer, we bred *Gclm*$^{+/-}$ mice with *MMTV-PyMT* mice, which develop spontaneous mammary tumors, to generate *MMTV-PyMT*;*Gclm*$^{-/-}$ mice (referred to as *PyMT-Gclm*$^{-/-}$ mice) (Guy et al., 1992). *PyMT-Gclm*$^{-/-}$ mice exhibited a significantly delayed mammary tumor onset compared to control *PyMT-Gclm*$^{+/+}$ (Figure 1A). Disruption of *Gclm* also resulted in reduced mammary tumor burden; at experimental endpoint, the total mass of tumors isolated from *PyMT-Gclm*$^{+/+}$ mice exceeded that from *PyMT-Gclm*$^{-/-}$ mice more than 2-fold (Figure 1B). Interestingly, a partial gene dosage effect was evident, as mammary tumor onset was delayed in *PyMT-Gclm*$^{+/-}$ mice, but no difference was ultimately observed in tumor burden at endpoint (Figures S1A and S1B available online). Histological analysis revealed that while all mammary tumors in control mice progressed to invasive ductal carcinoma (IDC), tumors in *PyMT-Gclm*$^{-/-}$ mice showed reduced proliferation and invasive progression (Figures 1C–1F). Furthermore, when IDC was observed in *PyMT-Gclm*$^{-/-}$ mice, it was much more focal in nature (data not shown). Next, we examined whether normal mammary gland development was impaired in *Gclm*$^{-/-}$ mice in order to account for any differences in tumorigenesis that could be attributed to a preexisting organ defect. No difference in ductal outgrowth was observed between *Gclm*$^{+/+}$ and *Gclm*$^{-/-}$ mice during mammary gland maturation (Figure S1C). Additionally, no gross differences in density of mammary branches were observed in *Gclm*$^{-/-}$ mice (Figure S1D). These results demonstrate that loss of *Gclm* impairs mammary tumor initiation and supports that any changes in tumorigenesis observed in *Gclm*$^{-/-}$ mice are directly linked to cancer outgrowth and not a preexisting defect in mammary glands.

To extend these findings beyond the context of mammary tumorigenesis, we examined the effect of loss of *Gclm* in two independent mouse models of spontaneous tumor development: *LSL-Kras*$^{G12D/+}$;*Trp53*$^{fl/fl}$ mice that develop sarcomas upon intramuscular injection of adenovirus encoding the Cre recombinase (Ad-Cre) (Kirsch et al., 2007), and *Pten*$^{+/-}$ mice, which develop lymphomas and thymomas (Suzuki et al., 1998). In both models, we observed a significantly reduced tumor burden in mice lacking *Gclm* (Figures 1G, 1H, and S1E–S1G). In support of these results, gene expression analysis shows *GCLM* to be upregulated across multiple human tumor types and prognostic data indicates that cancer patients with tumors having high *GCLM* mRNA have a lower probability of relapse-free survival and overall survival (Figures S1H and S1I). Together, these results show that depleted GSH synthesis, driven by loss of *GCLM*, impairs tumor initiation and progression.

Early Inhibition of GSH Synthesis, But Not Inhibition upon Tumor Onset, Impairs Tumorigenesis

Buthionine-[S, R]-sulfoximine (BSO) is a potent inhibitor of GSH synthesis (Griffith and Meister, 1979) (Figure S2) and oral delivery is an effective pharmacological model of continuous depletion of GSH levels in vivo (Watanabe et al., 2003). In an effort to examine whether chemical inhibition of GSH synthesis could mirror genetic inhibition of GSH synthesis, we treated *PyMT-Gclm*$^{+/+}$ mice with BSO. Mice were treated at two different time points: immediately after weaning (4 weeks old; "early BSO"), or upon mammary tumor onset as assessed by palpation (~6–12 weeks old; "onset BSO"). Early BSO treatment dramatically reduced the mammary tumor burden in *PyMT-Gclm*$^{+/+}$ mice (Figure 2A). Histological analysis of mammary tumors resected from early BSO mice revealed reduced proliferation and fewer instances of invasive carcinomas (Figures 2B and 2C), replicating the phenotype of *PyMT-Gclm*$^{-/-}$ mice. Intriguingly, when BSO was delivered upon mammary tumor onset, tumor burden was unchanged; as was tumor histology (Figures 2A–2C). These findings were also observed in sarcomas from the *LSL-Kras*$^{G12D/+}$;*Trp53*$^{fl/fl}$ Ad-Cre mice treated with BSO at early and onset time points (Figure 2D). To examine the temporal impact of BSO on ROS levels within the tumors, we measured the amount of oxidized DNA product 8-hydroxy-2′-deoxyguanosine

(F) Pathological classifications of tumors from the mice in (B). DCIS, ductal carcinoma in situ; IDC, invasive ductal carcinoma.
(G and H) Sarcomas (G) from *LSL-Kras*$^{G12D/+}$;*Trp53*$^{fl/fl}$ Ad-Cre *Gclm*$^{+/+}$ (n = 4) and *LSL-Kras*$^{G12D/+}$;*Trp53*$^{fl/fl}$ Ad-Cre *Gclm*$^{-/-}$ (n = 4) mice were resected and weighed, as were lymphomas (H) from *Pten*$^{+/-}$;*Gclm*$^{+/+}$ (n = 6) and *Pten*$^{+/-}$;*Gclm*$^{-/-}$ (n = 8) mice. Data are represented as mean ± SEM. P values were calculated using log-rank (Mantel-Cox) test (A) and unpaired t test (B, G, and H). ***p < 0.001; **p < 0.01.
See also Figure S1.

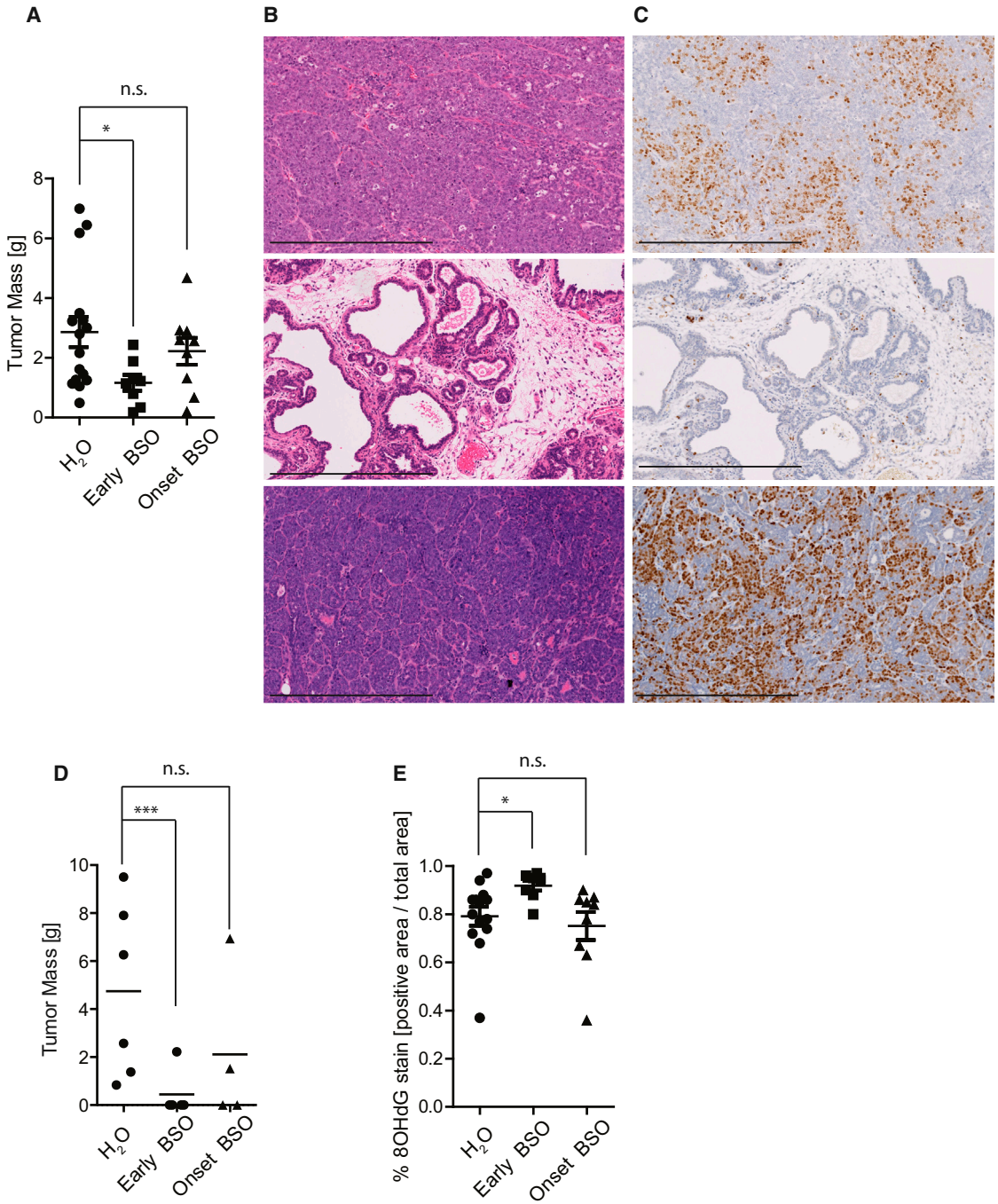

Figure 2. BSO Treatment Prevents Tumorigenesis

(A) At endpoint, tumors from H_2O controls (n = 16) and "early BSO" (n = 8) or "onset BSO" (n = 9) treated *PyMT-Gclm*$^{+/+}$ mice were resected and weighed.

(B and C) Representative images of sections of tumors from *PyMT-Gclm*$^{+/+}$ mice treated with H_2O (top), "early BSO" (middle) or "onset BSO" (bottom) stained with H&E (B) and Ki67 (C). Scale bars represent 400 μm.

(D) At endpoint, tumors from H_2O controls (n = 6) and "early BSO" (n = 5) or "onset BSO" (n = 4) treated *LSL-Kras*$^{G12D/+}$;*Trp53*$^{fl/fl}$ Ad-Cre *Gclm*$^{+/+}$ mice were resected and weighed.

(E) Quantification of percentage of 8OHdG staining in tumors from (A). Data are represented as mean ± SEM. P values were calculated using unpaired t test (A, D, and E). *$p < 0.05$; ***$p < 0.001$; n.s., nonsignificant.

See also Figure S2.

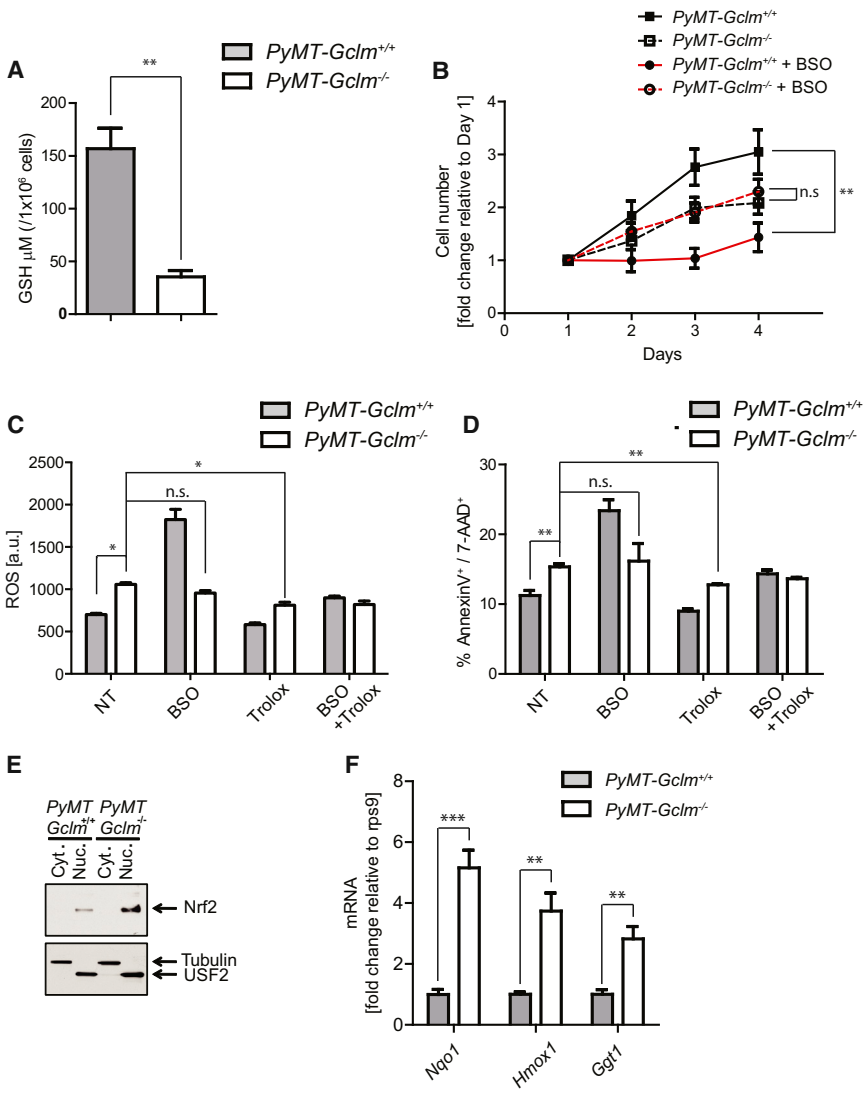

Figure 3. *PyMT-Gclm*$^{-/-}$ Cells Survive Inhibited GSH Synthesis

(A) Primary mammary epithelial cells (pMECs) from *PyMT-Gclm*$^{+/+}$ and *PyMT-Gclm*$^{-/-}$ mice were analyzed for total GSH levels (n = 3).

(B) *PyMT-Gclm*$^{+/+}$ and *PyMT-Gclm*$^{-/-}$ pMECs were cultured with or without BSO (150 μM) for the indicated times. Cell numbers expressed relative to the cell count on day 1 (n = 6).

(C and D) Cells from (B) were stained on day 3 for ROS levels (CM-H_2DCFDA) (C) and for apoptosis (AnnexinV, 7-AAD) (D) (n = 3).

(E) Immunoblotting of cytoplasmic (Cyt.) and nuclear (Nuc.) fractions of pMECs from *PyMT-Gclm*$^{+/+}$ and *PyMT-Gclm*$^{-/-}$ mice on day 4.

(F) Cells from (B) were harvested on day 4 and mRNA levels of the indicated Nrf2 target genes were determined by quantitative RT-PCR (qRT-PCR) (n = 6). *Nqo1*, NAD(P) dehydrogenase, quinone 1, *Hmox1*, heme oxygenase 1, *Ggt1*, gamma-glutamyltransferase 1. Data are represented as mean ± SEM. P values were calculated using unpaired t test (A, C, D, and F) and two-way ANOVA test (B). ***p < 0.001; **p < 0.01; *p < 0.05; n.s., nonsignificant.

(8OHdG) as a readout of ROS levels in vivo. Early BSO treatment, which reduced tumor burden, increased the amount of 8OHdG, while onset BSO treatment, which failed to reduce tumor burden, had no effect (Figure 2E). The increased 8OHdG staining in early BSO-treated tumors suggests that the ROS levels have accumulated to potentially produce an oxidative stress that can hinder the growth of the tumor. These results show that while inhibition of GSH synthesis is effective at allowing ROS levels to rise during the stage of tumor initiation, the same strategy has no effect on ROS levels in established tumors. This indicates that a potential reason for failure of BSO to impact the growth of established tumors is due to an alternate mechanism for depleting ROS at later stages of tumor progression.

GSH Synthesis Is Dispensable in Gclm Null Cells

To further investigate potential GSH-independent antioxidant responses of cancers, we isolated primary mammary epithelial cells (pMECs) from *PyMT-Gclm*$^{+/+}$ and *PyMT-Gclm*$^{-/-}$ mice. The GCLM subunit aides GCLC in producing de novo GSH; therefore loss of GCLM would be expected to decrease GSH synthesis without abolishing it completely. Accordingly, we observed greatly reduced, though still detectable, GSH levels in *PyMT-Gclm*$^{-/-}$ pMECs (Figure 3A). We postulated that *PyMT-Gclm*$^{-/-}$ pMECs would be more sensitive to cell death from BSO-mediated GSH inhibition due to their already decreased GSH levels. Although *PyMT-Gclm*$^{-/-}$ pMECs showed a reduction in cell growth rate, surprisingly, they were completely resistant to the effects of BSO (Figure 3B), suggesting that cells can compensate for further reduced GSH synthesis. The effects on cell growth corresponded with changes in both ROS levels and cell death and treatment with the antioxidant Trolox was able to rescue these effects (Figures 3C and 3D). To gain molecular insight into the potential driving force behind the response to glutathione depletion, we looked for evidence of upregulation of drivers of antioxidant gene expression. Nuclear factor (erythroid-derived 2)-like factor 2 (NFE2L2 or Nrf2) is a major antioxidant transcription factor that is stabilized upon oxidative stress; therefore we examined its levels and location in response to *Gclm* deletion. Interestingly, both protein stabilization of Nrf2 within the nucleus and Nrf2 target gene mRNA levels were increased in *PyMT-Gclm*$^{-/-}$ pMECs (Figures 3E and 3F). These results indicate that cells can survive loss of the GSH antioxidant pathway and this may potentially be mediated through Nrf2-dependent mechanisms.

Reduced GSH Synthesis Results in Increased Cystine Levels in Cells

In a continued effort to define the alternative mechanism for ROS reduction in BSO-treated cells, we examined the metabolites

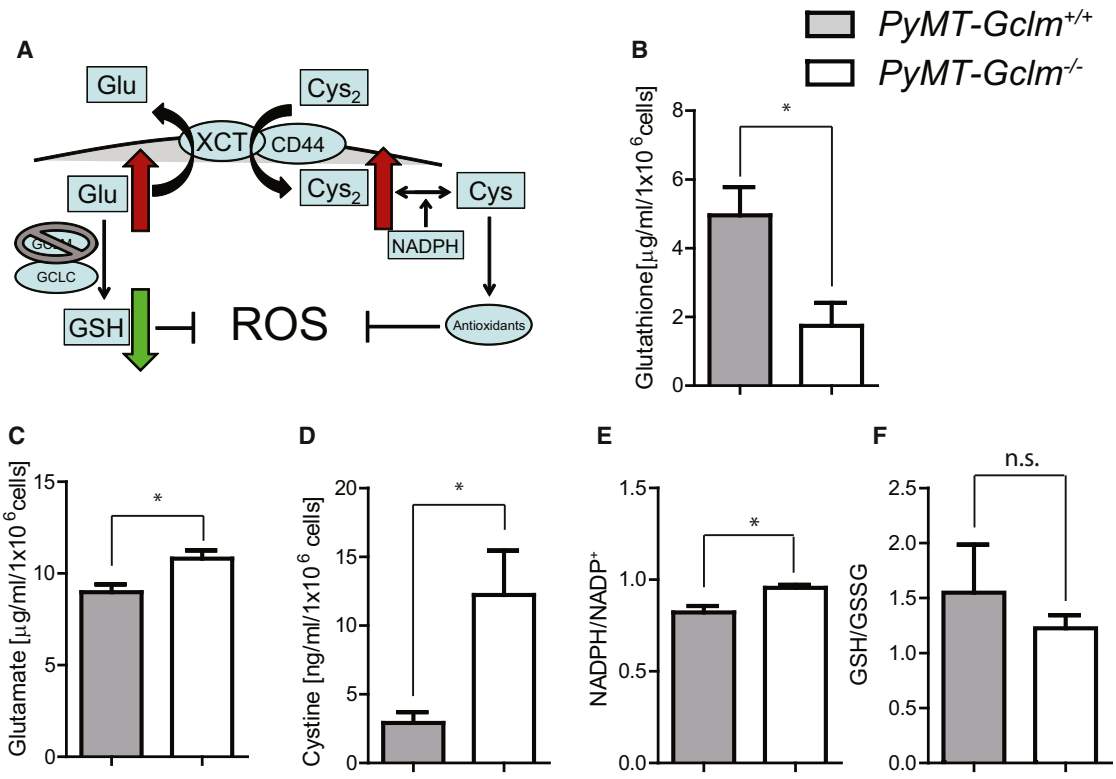

Figure 4. Inhibition of GSH Synthesis Results in Increased Intracellular Cystine Levels

(A) Schematic representation of antioxidant buffering provided by increased cystine import upon inhibition of de novo GSH synthesis. Glu, glutamate; Cys_2, cysteine.

(B–F) Quantitative metabolomics were performed to determine GSH (B), glutamate (C), and cystine (D) levels and NADPH/$NADP^+$ (E) and GSH/GSSG (F) ratios in pMECs from *PyMT-Gclm*$^{+/+}$ and *PyMT-Gclm*$^{-/-}$ mice (n = 4). Data are represented as mean ± SEM. P values were calculated using unpaired t test (B–F). *$p < 0.05$; n.s., nonsignificant.

involved in the synthesis of GSH. Glutamate, one of the substrates used by GCLM/GCLC to produce GSH, is required for the cellular import of cystine. Glutamate is exported from the cell in exchange for cystine via the amino acid transporter system Xc-, which features the XCT subunit (also known as SLC7A11) (Figure 4A) (Sasaki et al., 2002). Imported cystine, once reduced to cysteine in a NADPH-dependent manner, is incorporated into a multitude of antioxidant molecules. We reasoned that if GSH synthesis was inhibited, the excess glutamate that accumulated might be exported in exchange for the import of cystine. Accordingly, the increased cystine levels would be able to drive antioxidant synthesis to buffer ROS levels when GSH was depleted. To investigate this hypothesis, *PyMT-Gclm*$^{+/+}$ and *PyMT-Gclm*$^{-/-}$ pMECs were analyzed using quantitative metabolomics. In pMECs without *Gclm*, we observed decreased GSH levels, but increased glutamate and cystine levels (Figures 4B–4D). The metabolite NADPH regenerates oxidized GSH (GSSG) and its synthesis has been linked to oncogenic modifications and tumorigenesis (Vander Heiden et al., 2009). Interestingly, while we observe an increase NADPH/$NADP^+$ levels, no difference in GSH/GSSG levels was found (Figures 4E and 4F), suggesting that increased regeneration of GSH by NADPH is not occurring and is instead possibly used for cystine reduction. Overall, these results suggest that when GSH synthesis is reduced, increased intracellular cystine levels may drive an alternative antioxidant pathway.

Increased Expression of the TXN Antioxidant Pathway Occurs in GSH-Depleted Cells and Tumors

Previous reports had shown that overexpression of XCT can rescue the growth of cells that are completely deficient in GSH production, and this rescue was highly dependent upon the activity of the thioredoxin (TXN) antioxidant pathway (Mandal et al., 2010). Interestingly, mRNA of thioredoxin reductase 1 (TXNRD1) has been shown to be upregulated in the livers of *Gclm*$^{-/-}$ mice (Haque et al., 2010). The TXN pathway can efficiently reduce ROS levels and be regenerated by TXNRD in a GSH-independent manner (Holmgren and Lu, 2010). We postulated that increased expression of TXN pathway components could be facilitated by elevated cystine levels observed *PyMT-Gclm*$^{-/-}$ pMECs and could contribute to the mechanism by which GSH-depleted cells buffer ROS. In *PyMT-Gclm*$^{-/-}$ pMECs, we observed increases in the mRNA expression of several genes that promote the TXN antioxidant pathway and in the protein expression of Txn1 relative to *PyMT-Gclm*$^{+/+}$ pMECs (Figures 5A and 5B). Additionally, we found that the expression of the tumor-associated antigen CD44, which stabilizes XCT to promote cystine import, also increased in

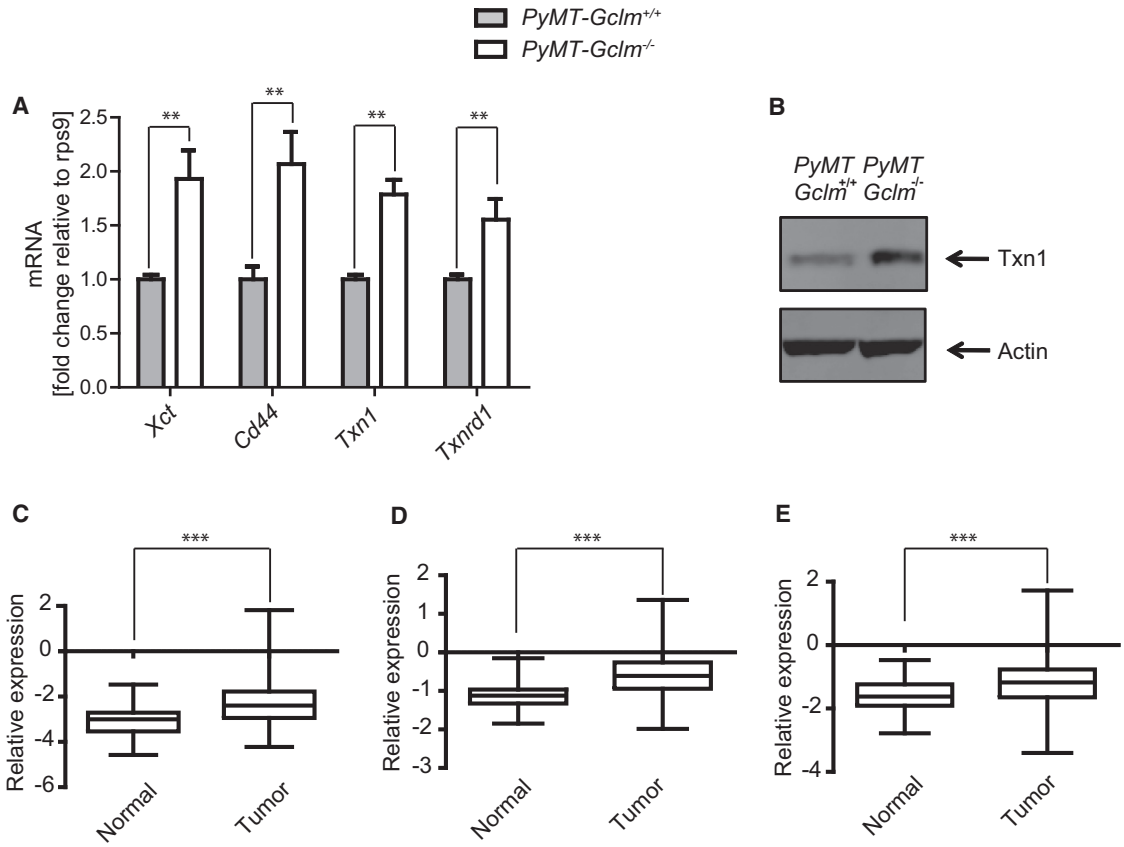

Figure 5. GSH-Depleted Cells and Tumors Upregulate the TXN Antioxidant Pathway

(A) pMECs from *PyMT-Gclm*$^{+/+}$ and *PyMT-Gclm*$^{-/-}$ mice were harvested and mRNA levels of the indicated genes were determined by qRT-PCR (n = 6).

(B) Immunoblotting of total lysate of pMECs from *PyMT-Gclm*$^{+/+}$ and *PyMT-Gclm*$^{-/-}$ mice.

(C–E) The mRNA levels of *XCT*, *TXN1*, and *TXNRD1* in the TCGA invasive breast carcinoma data set. Data are represented as mean ± SEM (A) and box and whiskers plots (C–E) with box defining 25th percentile (lower quartile), median and 75th percentile (upper quartile) and whiskers defining maximum and minimum values. P values were calculated using unpaired t test (A) Mann-Whitney U test (C–E). ***p < 0.001; **p < 0.01.

See also Figure S3.

PyMT-Gclm$^{-/-}$ pMECs (Figure 5A) (Ishimoto et al., 2011). In addition, we found that deletion of *Gclm* in mouse embryonic fibroblasts (MEF) and sarcomas from *Gclm*$^{-/-}$ *LSL-Kras*$^{G12D/+}$;*Trp53*$^{fl/fl}$ Ad-Cre mice upregulated TXN pathway-related gene expression, indicating that this effect is not limited to the mammary system (Figure S3). We hypothesized that if the TXN antioxidant pathway is upregulated in cancer cells compared to normal cells, this may help prime the tumor to survive GSH depletion. Indeed, examination of "The Cancer Genome Atlas" (TCGA) breast cancer data set revealed *XCT*, *TXN1*, and *TXNRD1* to be upregulated in breast cancer patient tissue compared to normal tissue (Figures 5C–5E) (Cancer Genome Atlas Network, 2012). These results suggest that the TXN pathway may compensate for inhibition of the GSH antioxidant pathway, and this alternative antioxidant pathway is elevated in established malignant tumors.

GSH and TXN Antioxidant Pathways Synergistically Support Cancer Cell Survival

In order to interrogate the reliance of cancer cells on the TXN antioxidant pathway when GSH synthesis was reduced, we utilized the chemical inhibitors sulfasalazine (SSA), which blocks the XCT transporter subunit and reduces cystine uptake (Gout et al., 2001), and auranofin (AUR), which reduces regeneration of TXN by inhibiting TXNRD (Marzano et al., 2007) (Figure 6A). Validation of both inhibitors showed robust and specific inhibition of the targeted pathways (Figures S4A–S4E). We chose to study the rapidly proliferating breast cancer cell line MDA-MB-231 to examine the coreliance on GSH and TXN antioxidant pathways in malignant cells. Treatment of cancer cells with BSO induced an increase in cystine uptake, identical to that observed with knockdown of *GCLM* (Figure 6B). While treatment with BSO, SSA, or AUR alone had minimal or no effect on the survival of cancer cells, combination of BSO with either SSA or AUR induced striking increases in cell death (Figures 6C and 6D). Cells depleted simultaneously of *GCLM* and *TXN* mRNA displayed reduced growth that matched chemical inhibition with BSO and SSA; they were also resistant to further growth inhibition by the chemicals (Figures S4F and S4G). Furthermore, the observed effects were dependent on increased ROS, as addition of Trolox or the antioxidant N-acetyl cysteine (NAC) was able to rescue the synergistic cell death

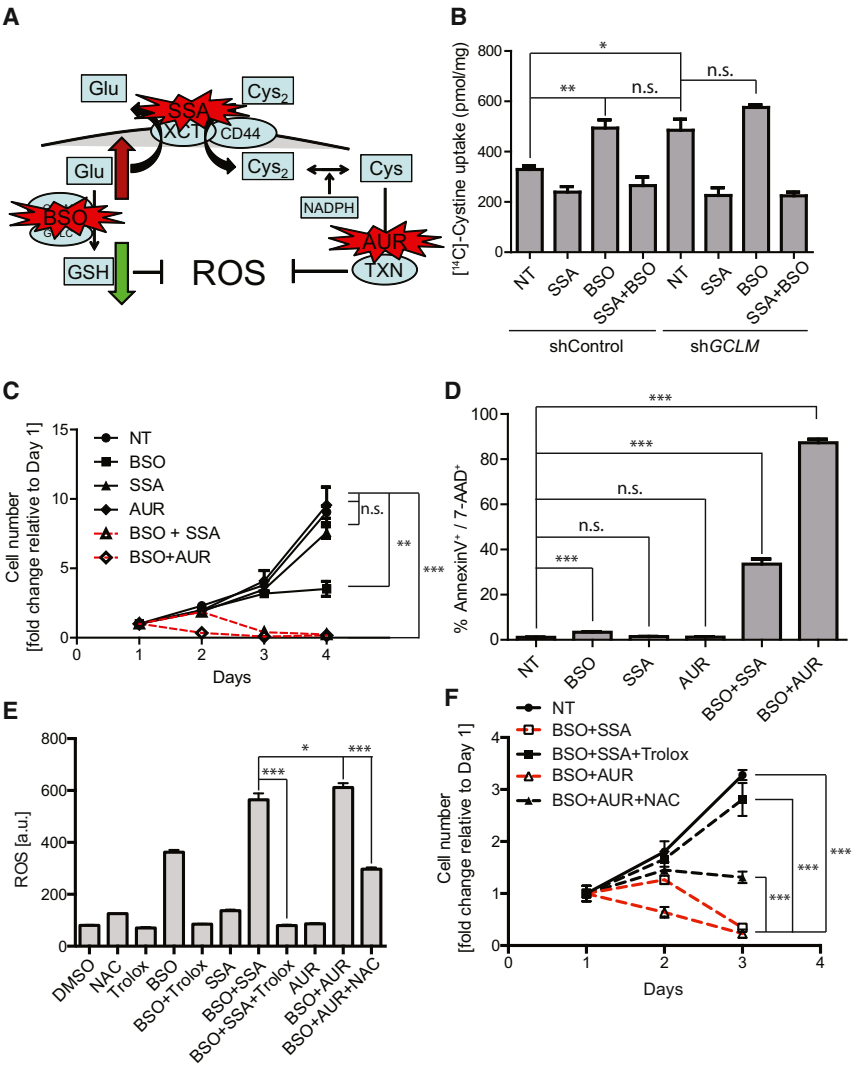

Figure 6. GSH and TXN Antioxidant Pathways Act in Synergy in Cancer Cells

(A) Schematic representation of target inhibition by BSO, SSA, and AUR.

(B) ^{14}C-Cystine uptake assay was performed on MDA-MB-231 cells expressing shControl or sh*GCLM* and not treated (NT) or treated with BSO (150 μM), SSA (250 μM), or both (n = 3).

(C) MDA-MB-231 cells were not treated (NT) or treated with BSO (150 μM), SSA (250 μM), or AUR (250 nM) alone or in the indicated combinations and cultured for indicated times. Cell numbers are expressed relative to cell count on day 1 (n = 3).

(D) Cells from (C) were analyzed on day 3 for apoptosis.

(E and F) ROS levels (E) and cell numbers (F) of MDA-MB-231 cells not treated (NT) or treated with BSO (150 μM), SSA (250 μM), AUR (250 nM), Trolox (250 μM), or NAC (1 mM) alone or in the indicated combinations and cultured for indicated times. ROS levels (E) were measured on day 2. Cell numbers are expressed relative to cell count on day 1 (n = 3). Data are represented as mean ± SEM. P values were calculated using unpaired t test (B, D, and E) and two-way ANOVA test (C and F). ***p < 0.001; **p < 0.01; *p < 0.05; n.s., nonsignificant.

See also Figure S4.

induced by BSO plus SSA or AUR (Figures 6E and 6F). Additionally, we observed similar phenotypes when examining cell lines from multiple different cancer types including lymphoma, glioblastoma, and nonsmall cell lung carcinoma (Figures S4H and S4I), suggesting that these in vitro findings were not limited to breast cancer cells. To investigate whether the GSH and TXN pathways synergize in vivo, we injected mice with MDA-MB-231 breast cancer cells and treated them with BSO, SSA, or both agents. While no effect on tumor growth was observed with administration of single agents, combined delivery of BSO and SSA synergistically reduced tumor growth in vivo (Figures 7A, 7B, and S5A). Corresponding results were found testing xenograft models using chemo-resistant patient-derived xenograft (PDX) and HCT116 colon cancer cells (Figures 7C, 7D, and S5B); again indicating that these findings may extend to other cancer types. Finally, cancer cells with combined depletion of *GCLM* and *TXN* mRNA showed reduced tumor burden in vivo that was matched and was not further exacerbated by treatment with BSO and SSA (Figures 7E and S5C). These results suggest that both GSH and TXN antioxidant pathways manage ROS levels in malignant tumors and, thus, combined inhibition of both pathways is required for effective induction of cancer cell death (Figure 8).

DISCUSSION

The role of antioxidants in tumorigenesis has been controversial for years. An overload of ROS within the cell leads to death, and the idea of inhibiting antioxidant pathways in order to kill cancer cells was first conceived long ago (Arrick et al., 1983). The concept that ROS can promote de novo mutagenesis arose almost concurrently and many believed that antioxidants could prevent or inhibit tumorigenic changes in preneoplastic cells (Bandy and Davison, 1990). Furthermore, later studies showed that ROS can mediate the activation of multiple signaling cascades that promote proliferation (Sena and Chandel, 2012). Activation of oncogenic pathways leads to increased production of ROS through numerous mechanisms (Cairns et al., 2011). The subsequent oxidative stress produced can promote signaling events, DNA damage, and mutagenesis and become a tumor promoter. If, however, this oxidative stress is not controlled, it can accumulate to higher levels that cause senescence or apoptosis and thus turn into a tumor suppressor. Recently, there has been a resurgence of evidence indicating that antioxidants contribute to tumorigenesis by preventing ROS accumulation and subsequent oxidative stress in cancer cells (DeNicola et al., 2011; Diehn et al., 2009; Schafer et al., 2009). Our results show that antioxidants, such as GSH, are required for cancer initiation and suggest that reduced antioxidant activity can in fact be chemopreventive. These findings are consistent with significantly increased cancer

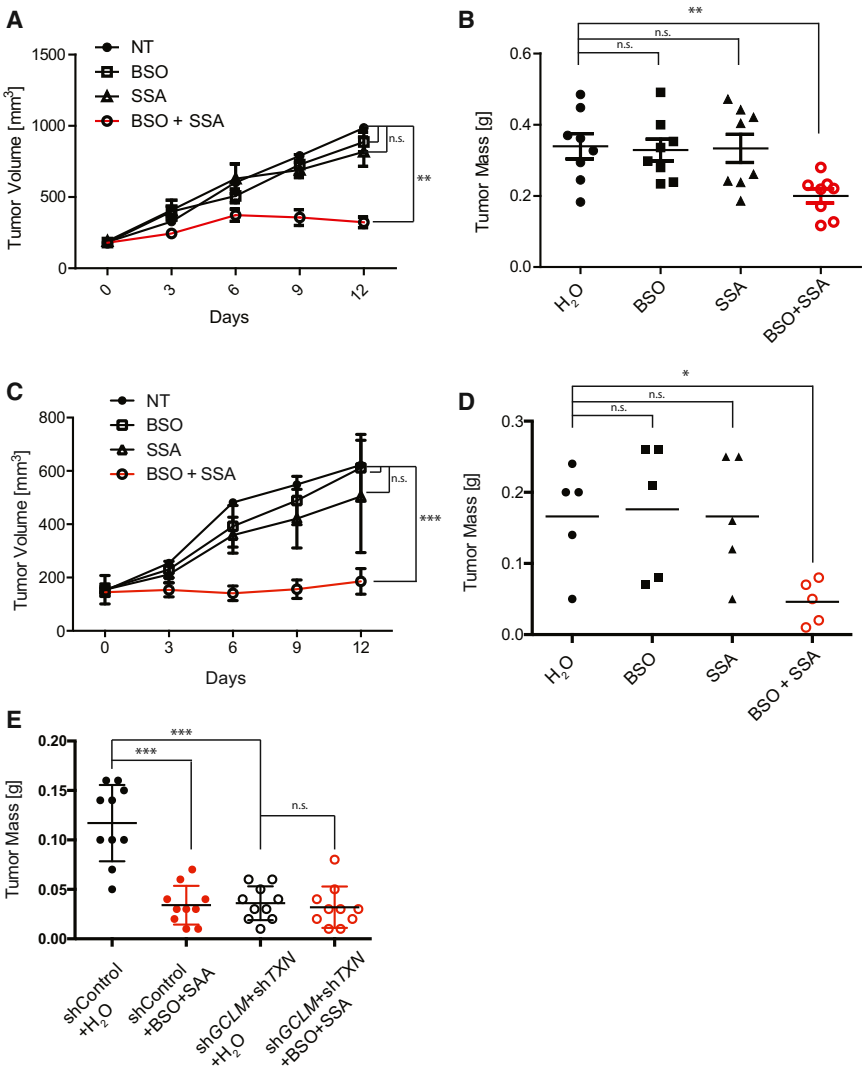

Figure 7. Combined Inhibition of GSH and TXN Antioxidant Pathways Synergistically Induces Cancer Cell Death In Vivo

(A) Tumor volume of SCID mice (n = 8/group) injected with MDA-MB-231 cells into the #4 fat pad and treated with H_2O, BSO, SSA, or BSO + SSA was monitored from initiation of drug treatment until endpoint (day 12).

(B) Tumors resected from mice in (A) at the end point were weighed.

(C) Tumor volume of SCID mice with subcutaneous transplantation of PDX treated with H_2O (n = 3), BSO (n = 5), SSA (n = 4), and BSO+SSA (n = 5) was monitored from initiation of drug treatment until endpoint (day 12).

(D) NIH III mice (n = 5/group) with hind flank injections of HCT116 cells were treated with H_2O, BSO, SSA, or BSO + SSA. At endpoint, each tumor was resected from each animal and tumor mass was determined.

(E) NIH III mice (n = 10/group) with hind flank injections of HCT116 cells expressing shControl or sh*GCLM* and sh*TXN* and treated with H_2O or BSO + SSA. At endpoint, each tumor was resected from each animal and tumor mass was determined. Data are represented as mean ± SEM. p values were calculated using two-way ANOVA test (A and C) and unpaired t test (B, D, and E). ***p < 0.001; **p < 0.01; *p < 0.05; n.s., nonsignificant.

See also Figure S5.

incidences observed in clinical trials that investigated whether antioxidants could prevent cancer (Klein et al., 2011; Omenn et al., 1996). These together suggest that not only caution should be exercised when using dietary antioxidant supplementation but also enzymes in antioxidant pathways may be legitimate targets for chemoprevention and cancer therapeutics (Gorrini et al., 2013).

Intriguingly, inhibition of the GSH pathway in an established malignant tumor did not significantly impede its progression. We hypothesize that reduction of ROS levels, in the presence of inhibited GSH synthesis, can specifically arise from the TXN antioxidant pathway due to increased cystine import, along with the increased expression of genes in this pathway found in malignant tumors. We postulate that the TXN antioxidant pathway can also be driven by the oncogenic transcription factor Nrf2, but further studies are required to validate this hypothesis. While our preliminary analysis focused on Nrf2, rescue for depleted antioxidants may also occur from other sources, such as p53, ATF, and FOXO families of transcription factors (Gutiérrez-Uzquiza et al., 2012; Nogueira et al., 2008; Rufini et al., 2012; Vousden and Ryan, 2009). Furthermore, although the study investigated the TXN antioxidant pathway, we cannot rule out that the increased cystine uptake that occurs in cells with reduced GSH synthesis may be diverted to other antioxidant pathways. A comprehensive examination of the mechanisms of antioxidant pathways in cancer cells would yield great insight toward understanding how interconnected antioxidant responses might support tumorigenesis.

GSH is the most abundant antioxidant in the cell, yet clinical trials targeted at inhibiting GSH synthesis alone have been met with little success (Bailey et al., 1997). Here, we demonstrate the capacity of cancer cells to survive a decrease in GSH synthesis by using the TXN antioxidant pathway to buffer ROS levels. This response is similar to that seen in oncogenic signaling pathways, such as when tumors become resistant to targeted therapies (Muranen et al., 2012). Combination therapy inhibiting both GSH and TXN antioxidant pathways may yield success when applied in the clinical setting. Interestingly, both SSA and AUR, which act synergistically with BSO to induce cancer cell death, are disease-modifying antirheumatic drugs (DMARDs) currently being used to treat inflammatory diseases (Möttönen et al., 1999); this underscores the realistic and potentially rapid clinical application of these findings. Further insight into the roles of other antioxidants, and how they act both alone and together, will no doubt provide important clues into more effective treatments for cancer patients.

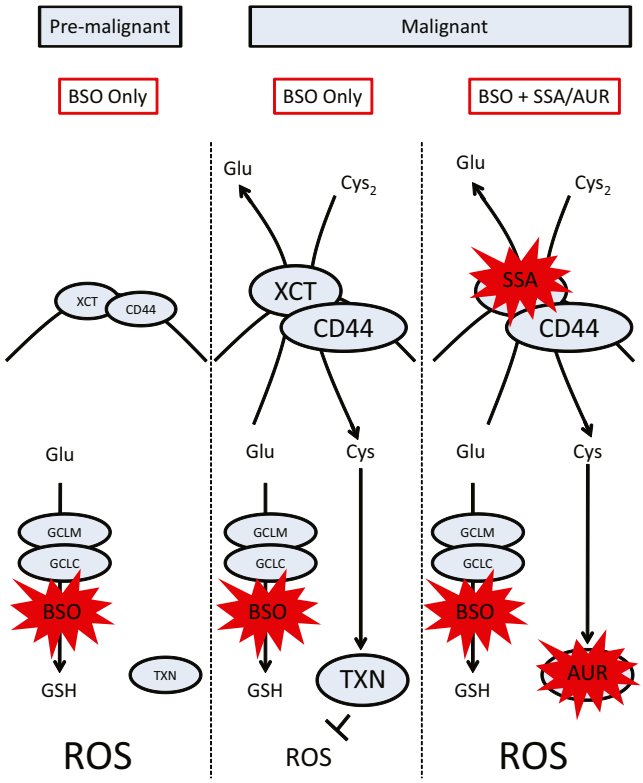

Figure 8. Treatment Strategies Involving Blockade of GSH and TXN Antioxidant Pathways in Malignant Tumors

Inhibition of GSH synthesis, through treatment with BSO, inhibits cancer initiation. If malignant transformation has already occurred, upregulation of alternative antioxidant pathways, including the TXN pathway, render treatment with BSO alone ineffective. Inhibition of both GSH and TXN pathways with combined delivery of BSO and SSA and/or AUR synergistically induces cancer cell death in established tumors.

EXPERIMENTAL PROCEDURES

Murine Tumor Models and Tumor Xenografts

MMTV-PyMT, *LSL-Kras*$^{G12D/+}$; *Trp53*$^{fl/fl}$, *Pten*$^{+/-}$, and *Gclm*$^{-/-}$ mice were generated as previously described (Guy et al., 1992; Kirsch et al., 2007; McConnachie et al., 2007; Suzuki et al., 1998) and kept on the identical genetic background. *PyMT-Gclm*$^{+/+}$ and *PyMT-Gclm*$^{-/-}$ mice (C57B6 background) were monitored weekly for palpable tumors, commencing at an age of 60 days. The experimental endpoint was defined as 160 days of age or if a humane endpoint was reached. At endpoint, all tumors from each individual mouse were resected and weighed. Data points represent a combined weight of tumors from a single mouse. Samples were divided in half, with one half being snap frozen at −80°C and the other half being fixed in 10% buffered formalin for use in histological analyses. Similar procedures were conducted for *LSL-Kras*$^{G12D/+}$;*Trp53*$^{fl/fl}$ Ad-Cre *Gclm*$^{+/+}$ and *LSL-Kras*$^{G12D/+}$;*Trp53*$^{fl/fl}$ Ad-Cre *Gclm*$^{-/-}$ mice (~8 weeks after Ad-Cre injection in skeletal muscle) and *Pten*$^{+/-}$;*Gclm*$^{+/+}$ and *Pten*$^{+/-}$;*Gclm*$^{-/-}$ mice (~6 months of age). *MMTV-PyMT* mice (129 background) were used for experiments involving continuous oral delivery of BSO (20 mM) and were performed as previously described (Watanabe et al., 2003). The experimental endpoint was 120 days of age or earlier if a humane endpoint was reached. Endpoints are earlier than in *MMTV-PyMT-C57B6* mice because the former animals develop tumors sooner. At endpoint, all tumors from each individual mouse were resected, weighed and divided into two samples for further analysis as described above. Data points represent a combined weight of tumors from a single mouse. Similar procedures were conducted for *LSL-Kras*$^{G12D/+}$;*Trp53*$^{fl/fl}$ Ad-Cre mice. Severe combined immunodeficiency (SCID) mice (n = 8/group) were injected into their #4 fat pads with 1 × 10^6 MDA-MB-231 cells in PBS with Matrigel. Mice were divided into four treatment cohorts: H_2O, untreated drinking water with daily intraperitoneal (i.p.) injection of vehicle control (0.9% NaCl solution); BSO, 20 mM BSO-treated drinking water with daily i.p. injection of vehicle control (0.9% NaCl solution); SSA, untreated drinking water with daily i.p. injection of SSA (250 mg/kg); BSO + SSA, 20 mM BSO-treated drinking water with daily i.p. injection of SSA (250 mg/kg). Tumor volumes were measured every 3 days until endpoint (day 12). At endpoint, tumors were excised, weighed, and processed for further analysis as described above. SCID mice (3–5/group) were subcutaneously transplanted with tumor fragments (2–3 mm) from a PDX model and then treated as previously mentioned with BSO and SSA. NIH III mice (n = 5–10/group) were subcutaneously injected with 1 × 10^6 HCT116 cancer cells (parental, shControl, or sh*GCLM*+sh*TXN*) and then treated as previously mentioned with BSO and SSA. The Institutional Animal Care and Use Committee (IACUC) of the University Health Network (UHN) approved all animal procedures. Animals were housed in the UHN Animal Resource Centre (fully accredited by the Canadian Council for Animal Care). The PDX model was generated from tumor tissue obtained from a consenting patient under a research protocol approved by the UHN Research Ethics Board (UHN REB#06-0196-CE).

Cells and Reagents

Isolation of pMECs was performed as previously described (Joshi et al., 2010). Each data point for experiments involving pMECs refer cells isolated from at least three separate mice and cultured separately. All pMECs were cultured for only one passage and maintained at 3% oxygen and in serum-free medium. Isolation of MEFs was performed as previously described (Inoue et al., 2013). All cancer cell lines were obtained from ATCC and cultured as specified. All reagents were obtained from Sigma-Aldrich, except for Trolox (Millipore).

Histology, Immunohistochemistry, and Pathological Analysis

Formalin-fixed tumor samples were processed and embedded in paraffin. Tissue sections (5 μm) were deparaffinized and stained with hematoxylin and eosin (H&E), Ki67, anti-smooth muscle actin antibody (Dako; M0851) or anti-8 hydroxyguanosine antibody [15A3] (Abcam; ab62623). Tumor slides stained for H&E and SMA, blinded and were evaluated by light microscopy and scored by two independent pathologists (S.J.D. and A.A.).

SUPPLEMENTAL INFORMATION

Supplemental Information includes Supplemental Experimental Procedures and five figures and can be found with this article online at http://dx.doi.org/10.1016/j.ccell.2014.11.019.

AUTHOR CONTRIBUTIONS

I.S.H., A.E.T., S. I., M.S., C.G., D.B., C.B.K.-T., M.A.C., D.W.C., A.B., W.Y.L., K.Y., and A.W. performed the majority of experiments. K.C.L., K.Y.Y., and C.W.L. performed quantitative metabolomics analysis. A.E. and T.B. performed histological analysis. S.D.M., J.M.M., and R.K. performed bioinformatics analysis. A.A., H.K.B., and S.J.D. performed pathological analysis. T.J.K. provided Gclm$^{-/-}$ mice. I.S.H., A.E.T., S. I., M.S., C.G., D.B., T.J.K., and T.W.M. wrote and edited the manuscript.

ACKNOWLEDGMENTS

We are very grateful for the generous gift of the Nrf2 antibody from Dr. Edward Schmidt (Montana State University). We would like to thank Mary Saunders, Jonathan L. Coloff, and Lisa L. Gallegos for scientific editing, Irene Ng for administrative help, and Marsha J. Barrett for discussions. This work was supported by a PGS-D grant from the Natural Sciences and Engineering Council of Canada (I.S.H.), a fellowship grant from the German Research Foundation (D.B.), funding by the ATTRACT program of the Luxembourg National Research Fund (D.B.), and a fellowship (I.S.H.) and grants (T.W.M.) from the Canadian Institutes of Health Research.

Received: March 18, 2013
Revised: July 15, 2014
Accepted: November 18, 2014
Published: January 22, 2015

REFERENCES

Arrick, B.A., Nathan, C.F., and Cohn, Z.A. (1983). Inhibition of glutathione synthesis augments lysis of murine tumor cells by sulfhydryl-reactive antineoplastics. J. Clin. Invest. *71*, 258–267.

Bailey, H.H., Ripple, G., Tutsch, K.D., Arzoomanian, R.Z., Alberti, D., Feierabend, C., Mahvi, D., Schink, J., Pomplun, M., Mulcahy, R.T., and Wilding, G. (1997). Phase I study of continuous-infusion L-S,R-buthionine sulfoximine with intravenous melphalan. J. Natl. Cancer Inst. *89*, 1789–1796.

Bandy, B., and Davison, A.J. (1990). Mitochondrial mutations may increase oxidative stress: implications for carcinogenesis and aging? Free Radic. Biol. Med. *8*, 523–539.

Cairns, R.A., Harris, I.S., and Mak, T.W. (2011). Regulation of cancer cell metabolism. Nat. Rev. Cancer *11*, 85–95.

Cancer Genome Atlas Network (2012). Comprehensive molecular portraits of human breast tumours. Nature *490*, 61–70.

Dalton, T.P., Dieter, M.Z., Yang, Y., Shertzer, H.G., and Nebert, D.W. (2000). Knockout of the mouse glutamate cysteine ligase catalytic subunit (Gclc) gene: embryonic lethal when homozygous, and proposed model for moderate glutathione deficiency when heterozygous. Biochem. Biophys. Res. Commun. *279*, 324–329.

DeNicola, G.M., Karreth, F.A., Humpton, T.J., Gopinathan, A., Wei, C., Frese, K., Mangal, D., Yu, K.H., Yeo, C.J., Calhoun, E.S., et al. (2011). Oncogene-induced Nrf2 transcription promotes ROS detoxification and tumorigenesis. Nature *475*, 106–109.

Diehn, M., Cho, R.W., Lobo, N.A., Kalisky, T., Dorie, M.J., Kulp, A.N., Qian, D., Lam, J.S., Ailles, L.E., Wong, M., et al. (2009). Association of reactive oxygen species levels and radioresistance in cancer stem cells. Nature *458*, 780–783.

Gorrini, C., Harris, I.S., and Mak, T.W. (2013). Modulation of oxidative stress as an anticancer strategy. Nat. Rev. Drug Discov. *12*, 931–947.

Gout, P.W., Buckley, A.R., Simms, C.R., and Bruchovsky, N. (2001). Sulfasalazine, a potent suppressor of lymphoma growth by inhibition of the x(c)- cystine transporter: a new action for an old drug. Leukemia *15*, 1633–1640.

Griffith, O.W., and Meister, A. (1979). Potent and specific inhibition of glutathione synthesis by buthionine sulfoximine (S-n-butyl homocysteine sulfoximine). J. Biol. Chem. *254*, 7558–7560.

Gutiérrez-Uzquiza, Á., Arechederra, M., Bragado, P., Aguirre-Ghiso, J.A., and Porras, A. (2012). p38α mediates cell survival in response to oxidative stress via induction of antioxidant genes: effect on the p70S6K pathway. J. Biol. Chem. *287*, 2632–2642.

Guy, C.T., Cardiff, R.D., and Muller, W.J. (1992). Induction of mammary tumors by expression of polyomavirus middle T oncogene: a transgenic mouse model for metastatic disease. Mol. Cell. Biol. *12*, 954–961.

Hanahan, D., and Weinberg, R.A. (2000). The hallmarks of cancer. Cell *100*, 57–70.

Haque, J.A., McMahan, R.S., Campbell, J.S., Shimizu-Albergine, M., Wilson, A.M., Botta, D., Bammler, T.K., Beyer, R.P., Montine, T.J., Yeh, M.M., et al. (2010). Attenuated progression of diet-induced steatohepatitis in glutathione-deficient mice. Lab. Investig. *90*, 1704–1717.

Holmgren, A., and Lu, J. (2010). Thioredoxin and thioredoxin reductase: current research with special reference to human disease. Biochem. Biophys. Res. Commun. *396*, 120–124.

Inoue, S., Hao, Z., Elia, A.J., Cescon, D., Zhou, L., Silvester, J., Snow, B., Harris, I.S., Sasaki, M., Li, W.Y., et al. (2013). Mule/Huwe1/Arf-BP1 suppresses Ras-driven tumorigenesis by preventing c-Myc/Miz1-mediated down-regulation of p21 and p15. Genes Dev. *27*, 1101–1114.

Ishimoto, T., Nagano, O., Yae, T., Tamada, M., Motohara, T., Oshima, H., Oshima, M., Ikeda, T., Asaba, R., Yagi, H., et al. (2011). CD44 variant regulates redox status in cancer cells by stabilizing the xCT subunit of system xc(-) and thereby promotes tumor growth. Cancer Cell *19*, 387–400.

Joshi, P.A., Jackson, H.W., Beristain, A.G., Di Grappa, M.A., Mote, P.A., Clarke, C.L., Stingl, J., Waterhouse, P.D., and Khokha, R. (2010). Progesterone induces adult mammary stem cell expansion. Nature *465*, 803–807.

Kirsch, D.G., Dinulescu, D.M., Miller, J.B., Grimm, J., Santiago, P.M., Young, N.P., Nielsen, G.P., Quade, B.J., Chaber, C.J., Schultz, C.P., et al. (2007). A spatially and temporally restricted mouse model of soft tissue sarcoma. Nat. Med. *13*, 992–997.

Klein, E.A., Thompson, I.M., Jr., Tangen, C.M., Crowley, J.J., Lucia, M.S., Goodman, P.J., Minasian, L.M., Ford, L.G., Parnes, H.L., Gaziano, J.M., et al. (2011). Vitamin E and the risk of prostate cancer: the Selenium and Vitamin E Cancer Prevention Trial (SELECT). JAMA *306*, 1549–1556.

Mandal, P.K., Seiler, A., Perisic, T., Kölle, P., Banjac Canak, A., Förster, H., Weiss, N., Kremmer, E., Lieberman, M.W., Bannai, S., et al. (2010). System x(c)- and thioredoxin reductase 1 cooperatively rescue glutathione deficiency. J. Biol. Chem. *285*, 22244–22253.

Marzano, C., Gandin, V., Folda, A., Scutari, G., Bindoli, A., and Rigobello, M.P. (2007). Inhibition of thioredoxin reductase by auranofin induces apoptosis in cisplatin-resistant human ovarian cancer cells. Free Radic. Biol. Med. *42*, 872–881.

McConnachie, L.A., Mohar, I., Hudson, F.N., Ware, C.B., Ladiges, W.C., Fernandez, C., Chatterton-Kirchmeier, S., White, C.C., Pierce, R.H., and Kavanagh, T.J. (2007). Glutamate cysteine ligase modifier subunit deficiency and gender as determinants of acetaminophen-induced hepatotoxicity in mice. Toxicol. Sci. *99*, 628–636.

Meister, A. (1983). Selective modification of glutathione metabolism. Science *220*, 472–477.

Möttönen, T., Hannonen, P., Leirisalo-Repo, M., Nissilä, M., Kautiainen, H., Korpela, M., Laasonen, L., Julkunen, H., Luukkainen, R., Vuori, K., et al. (1999). Comparison of combination therapy with single-drug therapy in early rheumatoid arthritis: a randomised trial. FIN-RACo trial group. Lancet *353*, 1568–1573.

Muranen, T., Selfors, L.M., Worster, D.T., Iwanicki, M.P., Song, L., Morales, F.C., Gao, S., Mills, G.B., and Brugge, J.S. (2012). Inhibition of PI3K/mTOR leads to adaptive resistance in matrix-attached cancer cells. Cancer Cell *21*, 227–239.

Nogueira, V., Park, Y., Chen, C.C., Xu, P.Z., Chen, M.L., Tonic, I., Unterman, T., and Hay, N. (2008). Akt determines replicative senescence and oxidative or oncogenic premature senescence and sensitizes cells to oxidative apoptosis. Cancer Cell *14*, 458–470.

Omenn, G.S., Goodman, G.E., Thornquist, M.D., Balmes, J., Cullen, M.R., Glass, A., Keogh, J.P., Meyskens, F.L., Valanis, B., Williams, J.H., et al. (1996). Effects of a combination of beta carotene and vitamin A on lung cancer and cardiovascular disease. N. Engl. J. Med. *334*, 1150–1155.

Rufini, A., Niklison-Chirou, M.V., Inoue, S., Tomasini, R., Harris, I.S., Marino, A., Federici, M., Dinsdale, D., Knight, R.A., Melino, G., and Mak, T.W. (2012). TAp73 depletion accelerates aging through metabolic dysregulation. Genes Dev. *26*, 2009–2014.

Sasaki, H., Sato, H., Kuriyama-Matsumura, K., Sato, K., Maebara, K., Wang, H., Tamba, M., Itoh, K., Yamamoto, M., and Bannai, S. (2002). Electrophile response element-mediated induction of the cystine/glutamate exchange transporter gene expression. J. Biol. Chem. *277*, 44765–44771.

Schafer, Z.T., Grassian, A.R., Song, L., Jiang, Z., Gerhart-Hines, Z., Irie, H.Y., Gao, S., Puigserver, P., and Brugge, J.S. (2009). Antioxidant and oncogene rescue of metabolic defects caused by loss of matrix attachment. Nature *461*, 109–113.

Sena, L.A., and Chandel, N.S. (2012). Physiological roles of mitochondrial reactive oxygen species. Mol. Cell *48*, 158–167.

Suzuki, A., de la Pompa, J.L., Stambolic, V., Elia, A.J., Sasaki, T., del Barco Barrantes, I., Ho, A., Wakeham, A., Itie, A., Khoo, W., et al. (1998). High cancer susceptibility and embryonic lethality associated with mutation of the PTEN tumor suppressor gene in mice. Curr. Biol. *8*, 1169–1178.

Trachootham, D., Zhou, Y., Zhang, H., Demizu, Y., Chen, Z., Pelicano, H., Chiao, P.J., Achanta, G., Arlinghaus, R.B., Liu, J., and Huang, P. (2006).

Selective killing of oncogenically transformed cells through a ROS-mediated mechanism by beta-phenylethyl isothiocyanate. Cancer Cell *10*, 241–252.

Trachootham, D., Alexandre, J., and Huang, P. (2009). Targeting cancer cells by ROS-mediated mechanisms: a radical therapeutic approach? Nat. Rev. Drug Discov. *8*, 579–591.

Vander Heiden, M.G., Cantley, L.C., and Thompson, C.B. (2009). Understanding the Warburg effect: the metabolic requirements of cell proliferation. Science *324*, 1029–1033.

Vousden, K.H., and Ryan, K.M. (2009). p53 and metabolism. Nat. Rev. Cancer *9*, 691–700.

Watanabe, T., Sagisaka, H., Arakawa, S., Shibaya, Y., Watanabe, M., Igarashi, I., Tanaka, K., Totsuka, S., Takasaki, W., and Manabe, S. (2003). A novel model of continuous depletion of glutathione in mice treated with L-buthionine (S,R)-sulfoximine. J. Toxicol. Sci. *28*, 455–469.

Wiseman, H., and Halliwell, B. (1996). Damage to DNA by reactive oxygen and nitrogen species: role in inflammatory disease and progression to cancer. Biochem. J. *313*, 17–29.